DOI: 10.30511/pcdp.2025.2060622.1025 - ISSN: 3060-8376 - Vol 2(2), 2025

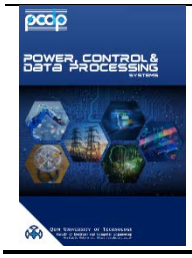

POWER, CONTROL AND DATA PROCESSING SYSTEMS

Available Online at: https://pcdp.qut.ac.ir/

Economic Operation of Multi-Carrier Microgrids Considering Energy Markets and Renewable Electricity Production

ARTICLE INFO

Article Type
Original Research

Authors
Sina Ahmadi[1]
Mehrdad Setayesh Nazar[2]

[1] Department of Electrical Engineering, Shahid Beheshti University, Tehran, Iran,
sina.ahmadi@mail.sbu.ac.ir
[2] Department of Electrical Engineering, Shahid Beheshti University, Tehran, Iran,
m_setayesh@mail.sbu.ac.ir

**** Correspondence***
Address: Department of Electrical Engineering, Shahid Beheshti University, Tehran, Iran.
Phone: -
Fax: -
sina.ahmadi@mail.sbu.ac.ir

Article History
Received: May 14, 2025
Accepted: May 22, 2025
ePublished: June 01, 2025

ABSTRACT

This study proposes a stochastic mixed-integer linear programming model for the optimal operation of a microgrid incorporating multiple energy carriers. Due to the inherent uncertainty in renewable energy generation, sudden high power generation from renewable sources may occur that the system cannot utilize directly. Nonetheless, these surplus energies can be transformed into other carriers. In this study, a probabilistic distribution function has been utilized to implement the stochastic model. The analysis results demonstrate that this approach effectively captures the stochastic behavior of the system. The research models and evaluates electric and hydrogen vehicle parking lots to assess their roles within the system. The approach is tested through two scenarios, demonstrating significant reductions in operational costs by effectively leveraging the sudden renewable energy surges. Operational costs for the first and second scenarios are 19,526 and 15,671 MU, respectively. A sensitivity analysis is also performed to confirm the robustness of the findings, ensuring the model's reliability under various conditions.

Keywords: Microgrid operation, energy markets, renewable resources, multi-carrier, and sudden energy production.

1 Introduction

Multi-carrier energy systems (MCESs) can convert one form of energy into another, enhancing their flexibility. This feature allows the system to supply energy from alternative sources in case of shortages and to convert excess production of one energy carrier into other carriers when capacity limits are exceeded. Consequently, these systems provide improved reliability and utilization of available resources. Numerous studies have been conducted by researchers in this domain. Ref [1] presents a day-ahead scheduling model for multi-carrier microgrids (MCMGs) integrating electricity, heating, cooling, gas, and hydrogen markets. Incorporating demand response and bi-directional communication between EV parking lots and hydrogen vehicle parking lots, the model employs stochastic MILP to handle uncertainties. Case studies demonstrate its effectiveness in reducing costs and enhancing system efficiency. Ref [2] evaluates the economic feasibility of deploying MCMGs, considering uncertainties, smart grid technologies, and demand response. It identifies optimal resource types, sizes, and deployment timing to ensure efficient and cost-effective system operation. Ref [3] presents a MILP model to optimize the selection, sizing, and dispatch of various energy sources, including electrical energy storage (EES), combined heat and power (CHP), thermal energy storage (TES), gas boiler (GB), and photovoltaic (PV). The system aims to reduce annual costs while enhancing resilience during prolonged outages, considering hourly energy demands. Ref [4] evaluates the technical and financial viability of a building-integrated multi-carrier energy hub for a large medical center. It proposes replacing high-exergy steam with district heating, integrating TES, cooling energy storage (CES), and PV generation to meet diverse energy demands efficiently. Ref [5] proposes a multi-objective model to optimize energy hubs and network design, reducing costs and emissions. It incorporates hydrogen energy in the topology and uses Monte Carlo and scenario analysis to evaluate wind and solar power outputs. Ref [6] introduces an efficient energy management algorithm for residential energy hubs, focused on optimizing costs and load profiles within a competitive market. The study proves the existence of a competitive equilibrium and proposes a linear scheduling approach to attain it, ensuring balanced and cost-effective operations. Ref [7] analyzes a community energy hub with integrated power-to-X(P2X) technology for hydrogen, heat, and methane, focusing on market participation and demand. In a 2050s climate scenario, the hub acts as both producer and consumer, promoting local renewables. P2X operation boosts renewable deployment, especially with low initial capacity, while seasonal storage remains secondary. It also reduces wholesale electricity trading volumes for the community. Ref [8] addresses the robust coordination of day-ahead and intra-day energy management under uncertainty, employing a distributionally robust, two-stage chance-constrained model. It optimizes bidding strategies and operational costs, ensuring flexible, resilient schedules for energy systems despite ambiguous data, with iterative re-dispatch for minimizing costs and balancing energy imbalances. Ref [9] introduces a risk-based bi-level model for integrating P2G units into a smart energy hub, balancing profit maximization and social welfare under renewable uncertainties. The model is linearized into MILP to facilitate practical implementation, optimizing cross-product arbitrage and market strategies. Ref [10] explores coordinated energy hub management across multiple networks through day-ahead market cooperation. It links electrical, natural gas, and district heating systems, utilizing CHP, storage, GB, electric vehicle parking lot (EVPL), and renewables to optimize integrated energy flows, enhancing system efficiency and flexibility. Ref [11] analyzes Denmark's reliance on wind and CHP, highlighting the challenge of surplus electricity during periods of excess generation. It discusses national strategies to address this imbalance, such as energy storage, grid integration, and flexible demand solutions, to ensure stable supply amid fluctuating renewable outputs. Ref [12] proposes an optimized dispatch strategy for integrated energy systems with CHP, renewables, and storage, utilizing a linear gas flow model with GSF matrices for computational efficiency. Incorporating gas network constraints and TES reduces operating costs from $384,098 to $378,430, enhancing flexibility, efficiency, and peak load management with EVPLs.

This paper introduces a comprehensive framework for the simultaneous planning of electricity markets, heating, cooling, gas, and hydrogen systems. It also proposes a solution for utilizing sudden energy surges generated by renewable sources, such as wind gusts. The instantaneous electrical energy produced can be converted into other energy carriers depending on system capabilities, enabling efficient utilization and preventing waste while also providing support for system loads within operational constraints. Additionally, this converted energy can be sold to upstream markets. The framework facilitates energy exchange between EVPL and hydrogen vehicle parking lot (HVPL). The proposed structure is flexible, allowing for interchanges among different energy carriers. In summary, the key innovations presented in this article include:

- Presentation of a new operational framework that accommodates multiple energy carriers.
- Conversion of sudden renewable energy surges into alternative energy carriers.
- Introduction of a new stochastic operational model that considers market prices, system demands, and the energy contributions from electric vehicles and hydrogen parking facilities.

In the upcoming sections, Section 2 will detail the proposed approach, Section 3 will present the simulation outcomes, and Section 4 will offer the conclusions.

2 Proposed method

A linear optimization model has been developed to minimize the operating costs of an MCMG, considering the sudden production of renewable energy sources. The proposed model was implemented and solved using GAMS software with the CPLEX method. The simulation outputs include the generation capacities of equipment, the charging and discharging levels of storage, and the energy exchanged with the upstream grid. Additionally, it shows the amount of energy accepted from proposed EVPL and HVPL facilities. Since the owner's primary goal is to reduce economic costs, the model prefers to utilize the energy generated by sudden renewable sources, such as high wind speeds and abrupt wind turbine (WT) outputs, to minimize the system's overall cost. The proposed operational framework is illustrated in Figure 1.

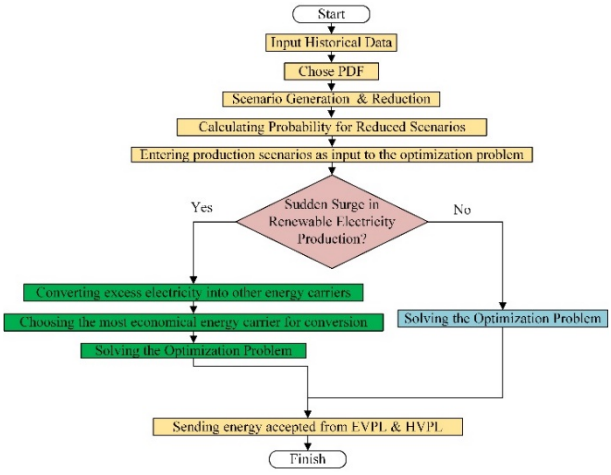

Figure 1. Flowchart of proposed method.

As mentioned, the decision variables of the optimization problem include the amounts of electricity and hydrogen exchanged with the upstream network, system components' outputs, and the accepted values from EVPL and HVPL. The proposed model includes constraints such as the capacities of branch connections with the upstream networks, EVPL, and HVPL; the generation levels of system equipment; storage operation limits; and the balance between the production and consumption of energy carriers. The objective function aims to minimize operating costs, representing the goal of the operator.

Figure 2 depicts the structure of the proposed model, which must supply the MG's demands, including electrical, thermal, cooling, gas, and hydrogen loads. Additionally, the system can exchange energy bidirectionally with the upstream grid, representing both buying and selling of energy. Storage units are incorporated for all energy carriers except gas storage. Given the system's design, it can convert between different energy carriers; for example, gas can be converted to hydrogen using a catalytic reactor (CR), and hydrogen can be converted into electricity and heat via a fuel cell (FC). This structure facilitates the energy transformation capabilities across all energy carriers within the system, enhancing flexibility and efficiency. Moreover, such a configuration allows for better integration of renewable sources and improves the resilience of the MG against supply fluctuations and demand variations.

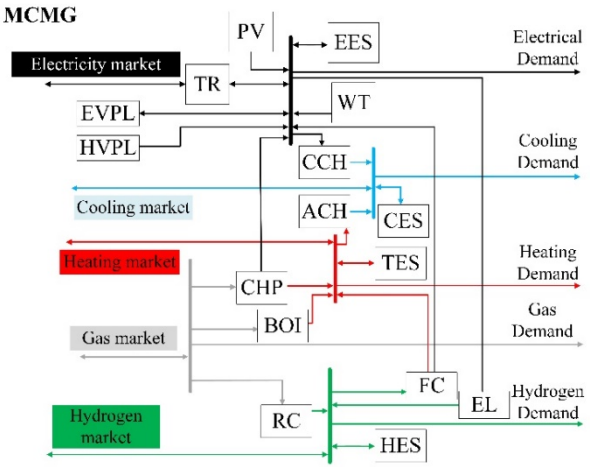

Figure 2. Topology of the MG system.

The MCMG operator (MCMGO) focuses on minimizing system costs by operating efficiently. To achieve this, it is crucial to identify the optimal operational states of the equipment and the amount of power exchanged with external entities. Equation (1) presents the objective function for normal operations, aiming to reduce the total operational costs over 24 hours. This function considers the costs related to energy exchanges with the upstream grid, EVPL, and HVPL, and its minimization depends on the market prices of energy. In this equation, the prices of electricity, thermal, cooling, gas, and hydrogen markets are expressed by parameters $\pi_{sc,t}^{Elec}$, $\pi_{sc,t}^{Ther}$, $\pi_{sc,t}^{Cool}$,$\pi_{sc,t}^{Gas}$, and $\pi_{sc,t}^{Hyd}$, respectively. The electrical, thermal, cooling, gas, and hydrogen energy exchanged with the upstream network are expressed as $P_{sc,t}^{G}$, $T_{sc,t}^{G}$, $C_{sc,t}^{G}$,$G_{sc,t}^{G}$, and$H_{sc,t}^{G}$, respectively. $P_{sc,t}^{EVPL}$ and $H_{sc,t}^{HVPL}$ are the electrical energy exchanged with EVPL and HVPL.

$$min\, F = \sum_{t=1}^{24}\sum_{sc=1}^{10}\frac{1}{\rho_s}(\pi_{sc,t}^{Elec}\cdot P_{sc,t}^{G} + \pi_{sc,t}^{Gas}\cdot G_{sc,t}^{G} + \pi_{sc,t}^{Cool}\cdot C_{sc,t}^{G} + \pi_{sc,t}^{Ther}\cdot T_{sc,t}^{G} + \pi_{sc,t}^{Hyd}\cdot H_{sc,t}^{G} + \pi_{sc,t}^{Elec}\cdot P_{sc,t}^{EVPL} + \pi_{sc,t}^{Elec}\cdot P_{sc,t}^{HVPL}) \quad \text{Eq 1}$$

In a MCMG, it is crucial to sustain a proper balance between energy generation and usage to ensure stability and sustainability. Achieving this balance enables optimal use of local resources and helps prevent overloads or power outages. By incorporating renewable energy sources (RES) and utilizing smart grid technologies, the MCMG can improve its resilience and adapt to variations in demand. The relationship between electrical energy supply and demand is represented in Equation (2). In this equation $P_{sc,t}^{CHP}$ is the electricity generation of CHP, $P_{sc,t}^{FC}$ is the electricity generation of FC, $P_{sc,t}^{PV}$ electricity generation of PV, $P_{c,t}^{WT}$ is the electricity generation of WT, $P_{sc,t}^{EES,dch}$and $P_{sc,t}^{EES,ch}$ are the electricity charge and discharge of ESS, respectively. The electrical demand of the system is specified by $P_{sc,t}^{Load}$ and $P_{sc,t}^{CCH}$ is equal to the electrical energy consumed by the CCH.

$$P_{sc,t}^{G} + P_{sc,t}^{CHP} + P_{sc,t}^{FC} + P_{sc,t}^{PV} + P_{sc,t}^{WT} + P_{sc,t}^{EVPL} + P_{sc,t}^{HVPL} + P_{sc,t}^{EES,dch} = P_{sc,t}^{CCH} + P_{sc,t}^{EES,ch} + P_{sc,t}^{Load} \quad \text{Eq 2}$$

Ensuring a proper balance between thermal and cooling energy is vital for optimizing energy efficiency within MCMGs. Proper management guarantees that thermal and cooling demands are satisfied efficiently, minimizing waste and improving overall system performance. Advanced control strategies play a key role in coordinating the generation and utilization of these energies effectively. Equations (3) and (4) illustrate the balance between thermal and cooling energy production and consumption, respectively. Achieving this balance is crucial for reducing operational costs and enhancing the sustainability of MCMG systems.

In this equation $T_{sc,t}^{CHP}$, $T_{sc,t}^{FC}$ and $T_{sc,t}^{GB}$ are the thermal energy produced by CHP, FC and GB, respectively. Charge and discharge of TES are indicated by $T_{sc,t}^{TES,ch}$ and $T_{sc,t}^{TES,dch}$, respectively. $T_{sc,t}^{Load}$ is a thermal demand and $T_{sc,t}^{ACH}$ is a thrmal energy consumption of ACH. In Equation (4) $C_{sc,t}^{CCH}$, $C_{sc,t}^{ACH}$, $C_{sc,t}^{CES,dch}$, $C_{sc,t}^{CES,ch}$ and $C_{sc,t}^{Load}$ are the cooling energy generation of CCH, cooling energy generation of ACH, discharging energy of CES, charging energy of CES and cooling demand, respectively.

$$T_{sc,t}^{G} + T_{sc,t}^{CHP} + T_{sc,t}^{FC} + T_{sc,t}^{GB} + T_{sc,t}^{TES,dch} = T_{sc,t}^{ACH} + T_{sc,t}^{TES,ch} + T_{sc,t}^{Load} \quad \text{Eq 3}$$

$$C_{sc,t}^{G} + C_{sc,t}^{CCH} + C_{sc,t}^{ACH} + C_{sc,t}^{CES,dch} = C_{sc,t}^{CES,ch} + C_{sc,t}^{Load} \quad \text{Eq 4}$$

Equality between gas and hydrogen production and consumption is another system requirement, as expressed in Equations (5) and (6), respectively. Gas purchased from the upstream network is consumed for CHP ($G_{sc,t}^{CHP}$), CR ($G_{sc,t}^{CR}$), GB ($G_{sc,t}^{GB}$), and load ($G_{sc,t}^{Load}$). Hydrogen produced by CR, hydrogen charged and discharged by the HES, hydrogen consumed by the FC, and hydrogen demand are marked as $H_{sc,t}^{CR}$, $H_{sc,t}^{HES,ch}$, $H_{sc,t}^{HES,dch}$, $H_{sc,t}^{FC}$, and $H_{sc,t}^{Load}$, respectively.

$$G_{sc,t}^{UP} = G_{sc,t}^{CHP} + G_{sc,t}^{CR} + G_{sc,t}^{GB} + G_{sc,t}^{Load} \quad \text{Eq 5}$$

$$H_{sc,t}^{UP} + H_{sc,t}^{CR} + H_{sc,t}^{HES,dch} = H_{sc,t}^{FC} + H_{sc,t}^{HES,ch} + H_{sc,t}^{Load} \quad \text{Eq 6}$$

The charging and discharging processes for all energy storage adhere to similar principles, each constrained by specific capacity limitations and technical restrictions. The comprehensive dynamic model for EES, TES, CES, and hydrogen storage (HES) is described in Equations (7) to (11), where the $u$index denotes the type of storage, whether EES, CES, HES, or TES. Similar constraints are also applied to each electric vehicle (EV) and hydrogen vehicle (HV), paralleling those used for the energy storages [13]. In this equation, $SOC_{sc,t}^{u}$ is the amount of stored energy, charging efficiency $\eta_{u,ch}$, $\eta_{u,dch}$ discharging efficiency, $E_{sc,t}^{u,ch}$ charging energy, $E_{sc,t}^{u,dch}$ discharging energy, $E_{max}^{u,ch}$ maximum charging energy, and $E_{max}^{u,dch}$ maximum discharging energy. $x_{sc,t}^{u}$ is a binary variable that indicates the battery charge status.

$$SOC_{sc,t}^{u} = SOC_{sc,t-1}^{u} + (E_{sc,t}^{u,ch}\eta_{u,ch} - \frac{E_{sc,t}^{u,dch}}{\eta_{u,dch}})\Delta t \quad \text{Eq 7}$$

$$0 \le E_{sc,t}^{u,ch} \le x_{sc,t}^{u} \cdot E_{max}^{u,ch} \quad \text{Eq 8}$$

$$0 \le E_{sc,t}^{u,dch} \le (1 - x_{sc,t}^{u}) \cdot E_{max}^{u,dch} \quad \text{Eq 9}$$

$$SOC_{min}^{u} < SOC_{SC,t}^{u} < SOC_{max}^{u} \quad \text{Eq 10}$$

$$SOC_{sc,0}^{u} = SOC_{sc,24}^{u} \quad \text{Eq 11}$$

The CHP system produces both electricity and heat by converting gas, operating with efficiencies denoted by η_{g2e}^{CHP} and η_{g2t}^{CHP}, respectively (as described in Equations (12) and (13)) [14]. The energy output from the system is limited by the specified constraints shown in Equations (14) and (15). To prevent equipment degradation associated with low-capacity operation, the system's operating range is maintained between 90% and 100% of its rated capacity, ensuring optimal performance and longevity. P_{max}^{CHP} and T_{max}^{CHP} are the electrical and thermal maximum nominal capacity of CHP [15]. Binary variable $I_{sc,t}^{CHP}$ indicates the commit status of this device.

$$P_{sc,t}^{CHP} = G_{sc,t}^{CHP} \times \eta_{g2e}^{CHP} \quad \text{Eq 12}$$

$$T_{sc,t}^{CHP} = G_{sc,t}^{CHP} \times \eta_{g2t}^{CHP} \quad \text{Eq 13}$$

$$0.9 I_{sc,t}^{CHP} \cdot P_{max}^{CHP} \le P_{sc,t}^{CHP} < I_{sc,t}^{CHP} \cdot P_{max}^{CHP} \quad \text{Eq 14}$$

$$0.9 I_{sc,t}^{CHP} \cdot T_{max}^{CHP} \le T_{sc,t}^{CHP} < I_{sc,t}^{CHP} \cdot T_{max}^{CHP} \quad \text{Eq 15}$$

In the model, an FC uses hydrogen to produce electricity and heat, offering an efficient energy conversion process that delivers clean power while also harnessing the heat produced as a useful thermal resource. Operating within defined performance parameters, the FC helps improve the overall efficiency of the system and supports sustainability objectives. The operational conditions and limitations of the FC are detailed in Equations (16) to (18) [1]. In this equation d the heat-to-power ratio of FC, ρ_{fc} is the hydrogen to electricity efficiency of FC, and P_{max}^{FC} is the maximum electricity generation of FC. Binary variable $I_{sc,t}^{FC}$ indicates the commit status of FC.

$$P_{sc,t}^{FC} = \rho_{fc} \cdot \eta_{h2e}^{FC} \cdot H_{sc,t}^{FC} \quad \text{Eq 16}$$

$$0 \le P_{sc,t}^{FC} \le I_{sc,t}^{FC} \cdot P_{max}^{FC} \quad \text{Eq 17}$$

$$T_{sc,t}^{FC} = \frac{1}{d} \cdot P_{sc,t}^{FC} \quad \text{Eq 18}$$

The gas boiler (GB) converts incoming gas into thermal energy to satisfy thermal needs, with its thermal output described in Equation (19). Similar to the CHP system, the GB operates within specific limits, governed by constraints outlined in Equation (20) [14]. In these equations, η_{g2t}^{GB} is the efficiency of converting gas energy into heat, T_{max}^{GB} is the maximum thermal energy that GB can produce, and $I_{sc,t}^{GB}$ is binary variable indicates the commitment of this equipment.

$$T_{sc,t}^{GB} = G_{sc,t}^{GB} \times \eta_{g2t}^{GB} \quad \text{Eq 19}$$

$$0.9 I_{sc,t}^{GB} \cdot T_{max}^{GB} \le T_{SC,t}^{GB} \le I_{SC,t}^{GB} \cdot T_{max}^{GB} \quad \text{Eq 20}$$

The CR is used for hydrogen production, converting gas into hydrogen. Its operational model and constraints are detailed in Equations (21) to (22) [1], [15]. η_{g2h}^{CR} is the efficiency of converting gas to hydrogen and H_{max}^{CR} is the max hydrogen that CR can generate. Binary variable $I_{sc,t}^{CR}$ indicates the commit status of this device.

$$H_{sc,t}^{CR} = G_{sc,t}^{CR} \times \eta_{g2h}^{CR} \quad \text{Eq 21}$$

$$0.5 I_{sc,t}^{CR} \cdot H_{max}^{CR} \le H_{SC,t}^{CR} \le I_{SC,t}^{CR} \cdot H_{max}^{CR} \quad \text{Eq 22}$$

In this study's MG framework, the ACH utilizes thermal energy from the heating hub to generate cooling energy. Its mathematical model, including the coefficient of performance (COP^{ACH}), is given in Equation (21). The cooling energy produced by the ACH is subject to constraints similar to those of the CHP, as shown in Equation (22). Likewise, the CCH follows models and constraints similar to the ACH, detailed in Equations (23) and (24) [13]. C_{max}^{ACH} and C_{max}^{CCH} are the max capacity generations of ACH and CCH, respectively. The commitment binary variable of these equipments is indicated by $I_{sc,t}^{CCH}$ and $I_{sc,t}^{ACH}$.

$$C_{sc,t}^{ACH} = COP^{ACH} \times T_{sc,t}^{ACH} \quad \text{Eq 22}$$

$$0.8I_{ss,t}^{ACH} \cdot C_{max}^{ACH} \leq C_{ss,t}^{ACH} \leq I_{ss,t}^{ACH} \cdot C_{max}^{ACH} \quad \text{Eq 23}$$

$$C_{sc,t}^{CCH} = COP^{CCH} \times P_{sc,t}^{CCH} \quad \text{Eq 24}$$

$$0.8I_{sc,t}^{CCH} \cdot C_{max}^{CCH} \leq C_{SC,t}^{CCH} \leq I_{SC,t}^{CCH} \cdot C_{max}^{CCH} \quad \text{Eq 25}$$

3 Simulation and Numerical Results

3.1 Solution Method

The exploitation strategy initially involves assigning a probabilistic distribution function to the uncertain parameters, including the electricity generation from photovoltaic systems, wind turbines, proposed electric and hydrogen parking capacities, and system demands and prices across different markets. Subsequently, based on Ref [1] and [15], probable scenarios are generated. Given the large number of resulting scenarios, which increases the problem's dimensionality, scenario reduction is necessary. Finally, probabilities are computed for the reduced set of scenarios. In the next step, considering whether there has been a sudden increase in wind speed, the MCMGO must assess how to convert this sudden surplus of energy into the most suitable carrier, while respecting system constraints to maximize profit. Additionally, the EVPL and HVPL operators submit their proposed values, which involve uncertainties, for the MCMGO to consider. After executing the optimization program, the accepted values will be determined. It is important to note that the communication with the HVPL operator involves only electrical energy exchange.

3.2 Input data and problem assumptions

The exchanged energy capacities with upstream networks are respectively 500, 500, 500, 800, and 800 kW for electrical, thermal, cooling, hydrogen, and gas networks. The electrical connection to the upstream grid is established via a transformer with an efficiency of 1. Information regarding the uncertain parameters can be obtained from Ref [16]. An exponential distribution function is used for the proposed capacities of the EVPL. Additionally, a normal distribution is employed for the proposed positive electrical values, representing the sale of electrical energy. The number of electric and hydrogen parking vehicles is 18 and 12, respectively, each exhibiting unique behaviors. The scenario generation for the proposed capacities of EVPL and HVPL, similar to other uncertain parameters. The reduced number of scenarios per uncertain parameter is set to 10. The average reduced scenario values are presented in Figures 3 to 5. Technical information regarding the system equipment is available in Ref [1].

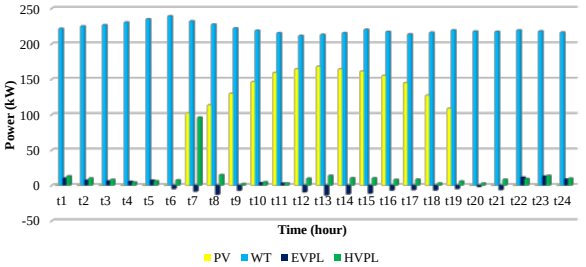

Figure 3. Average scenarios of PV, WT, EVPL and HVPL.

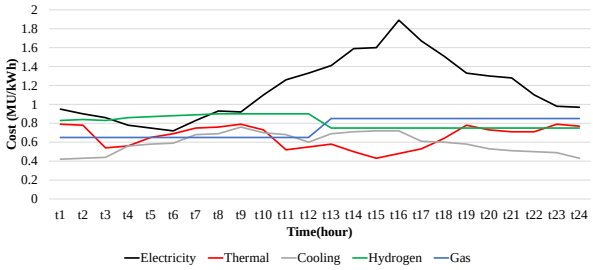

Figure 4. Average scenarios of electricity, heating, cooling, gas and hydrogen market prices.

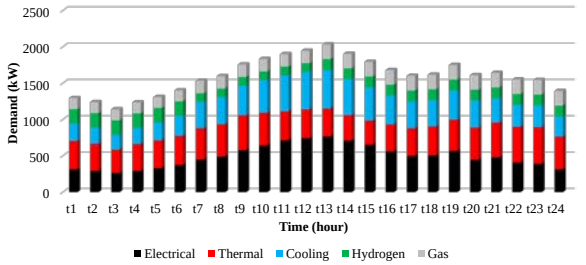

Figure 5. Average scenarios of electricity, heating, cooling, gas and hydrogen demand.

Furthermore, Figure 6 illustrates the electrical energy produced by the wind turbines following a sudden increase in wind speed.

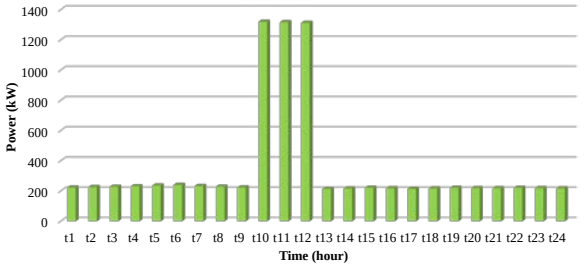

Figure 6. Power generation of WT in Case 2.

3.3 Case Studies and Numerical Results

In this section, the simulation results have been thoroughly analyzed and examined. Two case studies are considered in this study. The first case study focuses on the operation of the system under normal conditions, while the second case study analyzes the operation considering the sudden generation in power caused by strong wind gusts on the WT.

In the first case study, which involves the operation of the system under normal conditions, the operator manages the system based on the available system components. Since the primary goal of the MCMGO is to minimize economic costs, the operational cost over a 24-hour period amounts to 19,526 MU. Figure 7 illustrates the electrical energy exchanged with the upstream grids. The quantity of energy exchanged depends on market prices: at lower prices, the operator acts as an energy buyer, whereas at higher prices, they act as an energy seller. The electricity exchange with the upstream grid results in a profit of 2524 MU for the MCMGO. The costs associated with energy exchange for heating, cooling, hydrogen, and gas are, respectively, 2,524, 3,187, 326, and 12,668 MU.

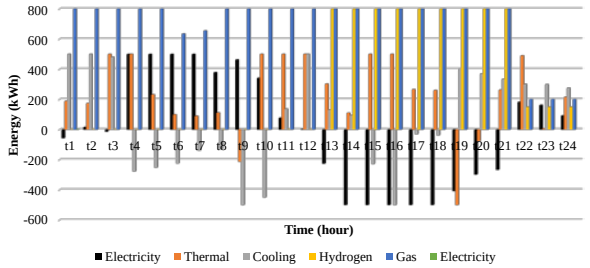

Figure 7. Exchanged energy with the upstream grids (Case 1).

Figure 8 depicts the electrical energy accepted from the ECPL and HVPL. This accepted energy amount depends on market prices and must be economically advantageous for the operator. The accepted electrical energy from the electric vehicle parking facility, based on purchase and sale transactions, is 43.1 kWh and 39.7 kWh, respectively. Additionally, the accepted electrical energy from the hydrogen vehicle parking facility over the operational period amounts to 150.7 kWh.

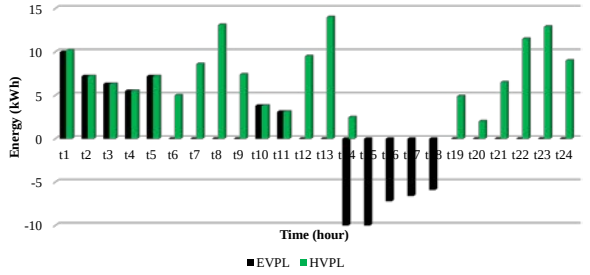

Figure 8. Accepted power from EVPL and HVPL (Case 1).

Figure 9 illustrates the electrical energy produced by the CHP and the FC. Considering the conversion coefficients, the thermal energy generated by these systems can also be calculated. The amount of electrical energy produced by the CHP system depends on various factors, including market prices for electricity, heat, and gas, as well as the conversion efficiencies of these systems. Among these factors, the most significant impact on the electrical energy output is the price difference between the electricity and gas markets. For example, during periods t1 to t5, when the gas market price is lower than the electricity market price, the system operates to produce electricity. The electrical energy generated by the fuel cell, influenced by market prices for electricity, heat, hydrogen, and the energy conversion coefficients, amounts to 3,269 kWh over the operational period.

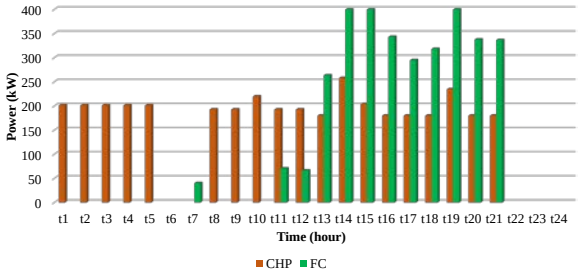

Figure 9. Electrical power generated by CHP and FC (Case 1).

Figure 10 illustrates the cooling energy produced by the ACH and CCH. During the operational period, the ACH and the ACH generate 3,600 kWh and 3,500 kWh of cooling energy, respectively. The energy output of these systems depends on market prices for cooling, electricity, and heating, and the MCMGO optimizes their operation accordingly to achieve cost-effective production.

Figure 11 displays the behavior of the energy storage systems. Since the operator's primary goal is to minimize economic costs, these systems act economically by charging during low-price periods and discharging during high-price periods.

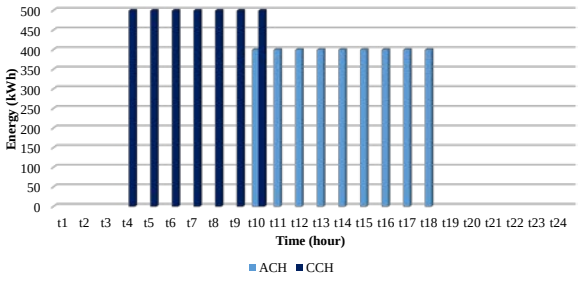

Figure 10. cooling energy produced by the ACH and CCH (Case 1).

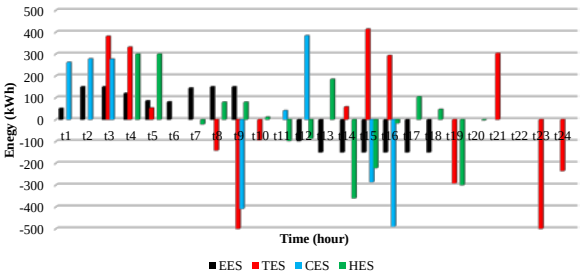

Figure 11. Behavior of the energy storage systems (Case 1).

In the second case study, during hours t10, t11, and t12, due to sudden wind gusts, the system's energy production increased significantly compared to the first case study, reaching 1,318 kW, 1,311 kW, and 1,315 kW, respectively, from previous values of 218, 215, and 211 kW. Considering the technical details of the MCMG, the capability for storage, consumption, or sale of this excess energy is limited. Therefore, the optimal approach is to utilize the existing capacity of the MCMG to convert this energy into other energy carriers. For example, the electrical energy can be transformed into hydrogen via an electrolyzer or into cooling energy through an ACH. Additionally, it can be sold to the upstream grid or stored in energy storage systems. The priority lies in how this excess energy is allocated, which depends on the prices of each energy carrier and the energy conversion efficiencies of the equipment. This sudden surge in energy production directly and indirectly influences other transactions and the energy outputs of the microgrid devices.

Table 1 presents the changes in the energy exchanged with the upstream grid, the energy produced by the equipment, and the charging and discharging behavior of the storage systems in both the first and second case studies. In this table, negative values for the markets indicate sales, while negative values for the storage systems indicate discharging. As observed, various changes have occurred. For example, the amount of natural gas purchased from the upstream grid has decreased during these hours, leading to a reduction in the system's overall operating costs. Additionally, the electrical energy produced by the CHP system has decreased in the second scenario. Moreover, the behavior of the CES has also changed accordingly.

Table 1. The quantity of energy transferred with the upstream grid and the operational cost for each case study

Case study	**SC1**			**SC2**		
Time	**t1**	**t2**	**t3**	**t1**	**t2**	**t3**
Gas	800	800	800	654	654	784
Cooling	-450	136	500	-500	-404	316
EES	0	0	-98.5	51.29	-9.48	150
Electricity	342	77	1.5	-500	-500	-500
EVPL	3.8	3.1	0	3.8	3.1	0
TES	-93.9	0	0	-13.63	36.3	-73.48
Thermal	500	500	500	500	500	500
CES	0	40.8	384	-50	0	700
ACH	400	400	400	400	400	400
CCH	500	0	0	500	500	500
CHP(P)	219	192	192	0	0	186
FC	0	70.2	66.2	0	0	0
H	0	0	0	0	0	0
HES	11	-97.29	-87.29	0	0	0
CR	131	200	200	200	200	200
Elctrolyzer	0	0	0	0	0	0

In the second scenario, since the electrical energy generated by the wind turbine incurs no operational costs, it is expected that the overall operating costs will decrease compared to the first scenario. The operating cost in the second scenario amounts to 15,671 MU, reflecting a reduction relative to the first scenario. This paper is organized into the following sections: The Introduction presents the background and motivation; the Proposed Method details the approach used; the Simulation and Numerical Results showcase the performance and validation; and the Conclusion summarizes the findings and offers final remarks.

4 Conclusion

This article presents an operational framework for a multi-energy carrier system, with the primary goal of minimizing operational costs for the operator. Two cases are analyzed in this study: the first case involves standard operation under normal conditions, and the second case considers operation accounting for sudden production from renewable sources. The comprehensive nature of the proposed model distinguishes it from other research efforts. Given the system's flexibility in converting one energy carrier into others, it has the capacity to transform the sudden energy surges from renewable sources into different forms of energy. However, due to system limitations, this excess energy can only be converted into other energy carriers. The results demonstrate that utilizing the sudden energy production from wind turbines significantly reduces operational costs compared to the first case. Specifically, the operational costs for the first and second cases are 19,526 and 15,671 MU, respectively. For future work, electrical network constraints can be incorporated to make the model more realistic. Additionally, solving the proposed model using artificial intelligence tools may significantly increase the solution speed.

5 Acknowledgement

This research was supported/partially supported by [Name of Foundation, Grant maker, Donor]. We thank our colleagues from [Name of the supporting institution] who provided insight and expertise that greatly assisted the research, although they may not agree with all of the interpretations/conclusions of this paper.

Disclosure of Potential Conflicts of Interest

The Authors declare that there is no conflict of interest

Reference

[1] [1] S. Ahmadi and M. S. Nazar, “Stochastic Day-Ahead Economic Operation Scheduling of Multi-Carrier Microgrids Considering Energy Markets and Demand Response,” in *2025 12th Iranian Conference on Renewable Energies and Distributed Generation (ICREDG)*, IEEE, 2025, pp. 1–6.

[2] [2] V. Amir and M. Azimian, “Dynamic multi-carrier microgrid deployment under uncertainty,” *Appl. Energy*, vol. 260, p. 114293, 2020.

[3] [3] H. Masrur, M. Shafie-Khah, M. J. Hossain, and T. Senjyu, “Multi-energy microgrids incorporating EV integration: Optimal design and resilient operation,” *IEEE Trans. Smart Grid*, vol. 13, no. 5, pp. 3508–3518, 2022.

[4] [4] J. Kalina and W. Pohl, “Technical and economic analysis of a multicarrier building energy hub concept with heating loads

at different temperature levels," *Energy*, vol. 288, p. 129882, 2024.

[5] [5] Q. Wu, M. Chen, H. Ren, Q. Li, and W. Gao, "Collaborative modeling and optimization of energy hubs and multi-energy network considering hydrogen energy," *Renew. Energy*, vol. 227, p. 120489, 2024.

[6] [6] F. Kamyab and S. Bahrami, "Efficient operation of energy hubs in time-of-use and dynamic pricing electricity markets," *Energy*, vol. 106, pp. 343–355, 2016.

[7] [7] Y. Wan, T. Kober, T. Schildhauer, T. J. Schmidt, R. McKenna, and M. Densing, "Conditions for profitable operation of p2x energy hubs to meet local demand with energy market access," *Adv. Appl. Energy*, vol. 10, p. 100127, 2023.

[8] [8] J. Cao, B. Yang, S. Zhu, C. Y. Chung, and X. Guan, "Multi-level coordinated energy management for energy hub in hybrid markets with distributionally robust scheduling," *Appl. Energy*, vol. 311, p. 118639, 2022.

[9] [9] A. Moradi, J. Salehi, and M. Shafie-khah, "An interactive framework for strategic participation of a price-maker energy hub in the local gas and power markets based on the MPEC method," *Energy*, vol. 307, p. 132608, 2024.

[10] [10] S. Gu, C. Rao, S. Yang, Z. Liu, A. U. Rehman, and M. A. Mohamed, "Day-Ahead market model based coordinated multiple energy management in energy hubs," *Sol. Energy*, vol. 262, p. 111877, 2023.

[11] [11] H. Lund and E. Münster, "Management of surplus electricity-production from a fluctuating renewable-energy source," *Appl. Energy*, vol. 76, no. 1–3, pp. 65–74, 2003.

[12] [12] H. Zaker, A. Rasouli, A. H. Alobaidi, and M. Sedighizadeh, "Optimal dispatch of multi-carrier energy system considering energy storage and electric vehicles," *J. Energy Storage*, vol. 90, p. 111794, 2024.

[13] [13] A. Bostan, M. S. Nazar, M. Shafie-Khah, and J. P. S. Catalão, "Optimal scheduling of distribution systems considering multiple downward energy hubs and demand response programs," *Energy*, vol. 190, p. 116349, 2020.

[14] [14] M. Armioun, M. S. Nazar, M. Shafie-khah, and P. Siano, "Optimal scheduling of CCHP-based resilient energy distribution system considering active microgrids' multi-carrier energy transactions," *Appl. Energy*, vol. 350, p. 121719, 2023.

[15] [15] S. Ahmadi;, M. M. Amiri;, M. S. Nazar;, and M. T. Ameli, "Day-ahead optimal scheduling for a energy hub operation considering markets for electricity, heat, cooling and gas," in *The 14th International Conference on Smart Grids*, https://sgc2024.khatam.ac.ir/en/, 2025.

[16] [16] S. Aghajan-Eshkevari, S. Azad, M. Nazari-Heris, M. T. Ameli, and S. Asadi, "Charging and discharging of electric vehicles in power systems: An updated and detailed review of methods, control structures, objectives, and optimization methodologies," *Sustainability*, vol. 14, no. 4, p. 2137, 2022.